A Nanonet-Enabled Li Ion Battery Cathode Material with High Power Rate, High Capacity, and Long Cycle Lifetime

Sa Zhou, Xiaogang Yang, Yongjing Lin, Jin Xie, and Dunwei Wang*

Department of Chemistry, Merkert Chemistry Center, Boston College, 2609 Beacon Street, Chestnut Hill, Massachusetts 02467, United States

ABSTRACT

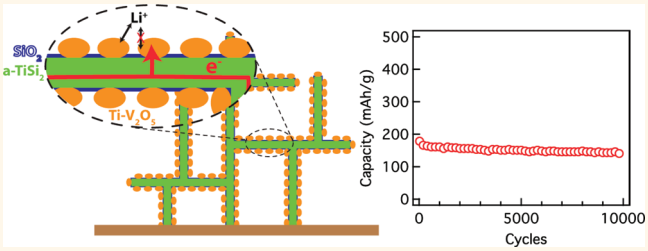

The performance of advanced energy conversion and storage devices, including solar cells and batteries, is intimately connected to the electrode designs at the nanoscale. Consider a rechargeable Li ion battery, a prevalent energy storage technology, as an example. Among other factors, the electrode material design at the nanoscale is key to realizing the goal of measuring fast ionic diffusion and high electronic conductivity, the inherent properties that determine power rates, and good stability upon repeated charge and discharge, which is critical to the sustainable high capacities. Here we show that such a goal can be achieved by forming heteronanostructures on a radically new platform we discovered, $TiSi_2$ nanonets. In addition to the benefits of high surface area, good electrical conductivity, and superb mechanical strength offered by the nanonet, the design also takes advantage of how $TiSi_2$ reacts with O_2 upon heating. The resulting $TiSi_2/V_2O_5$ nanostructures exhibit a specific capacity of 350 Ah/kg, a power rate up to 14.5 kW/kg, and 78.7% capacity retention after 9800 cycles of charge and discharge. These figures indicate that a cathode material significantly better than V_2O_5 of other morphologies is produced.

KEYWORDS: lithium ion battery · titanium disilicide · vanadium oxide · high power rate · long cycle time

Nanoscale materials are expected to contribute significantly to realizing an important goal in the lithium ion battery research of achieving high capacity *and* power rate and long cycle lifetime simultaneously.[1] Indeed, approaches to addressing one or more aspects of related issues separately using nanomaterials have been reported.[2−7] How to solve these issues in a concerted fashion, however, remains a challenge because they are intricately correlated at relevant length scales (*e.g.,* charge and ionic behaviors at the nanoscale). Here we present a strategy that has the potential to meet this challenge. Using the highly conductive two-dimensional $TiSi_2$ nanonet as a platform,[8] we obtained a V_2O_5-based cathode material through simple chemical synthesis. A specific capacity of 350 mAh/g, a power rate of 14.5 kW/kg, and a capacity retention of 78% after 9800 cycles of repeated charge/discharge were measured.

The key to our design (Figure 1) is the capability to control the features of materials on multiple levels concurrently. At the atomic scale, we use Ti-doping to stabilize V_2O_5 upon lithiation and delithiation,[9,10] which dramatically improves the cycle lifetime. At the nanoscale, the material is composed of more than one component, each designed for a specific function, the $TiSi_2$ nanonet for charge transport, the Ti-doped V_2O_5 nanoparticle as the ionic host, and the SiO_2 coating as a protection to prevent Li^+ from reacting with $TiSi_2$, which otherwise would lead to the destruction of the nanostructures. The strategy of having multiple components at the nanoscale offers a critical advantage of achieving desired electronic and ionic properties on the same material by tailoring the constituent components.[11] Our approach may be compared with previous methods of introducing inactive materials,[12] or with more recent treatments of including various nanostructures.[13−20] There are, however, at least three features to distinguish the system reported here. First, our two-dimensional $TiSi_2$ nanonet inorganic framework is highly unique. For instance, the combination of mechanical strength and flexibility exhibited by the nanonet may be ideal for energy storage applications.[8,21,22] Second,

* Address correspondence to dunwei.wang@bc.edu.

Received for review November 17, 2011 and accepted December 18, 2011.

Published online December 18, 2011
10.1021/nn204479n

without the involvement of catalysts or templates, the seemingly complex design as shown in Figure 1 is realized through simple chemical synthesis. Last and most important, the combined power rate, specific capacity, and cycle lifetime render our nanonet-based nanostructure one of the highest performing cathode materials.

RESULTS AND DISCUSSIONS

We are interested in using V_2O_5 to demonstrate the design principle because the addition of a conductive framework ($TiSi_2$ nanonets) is particularly useful to solve the key issues of poor conductivity and slow Li^+ diffusion that limit the performance of V_2O_5.[23] The

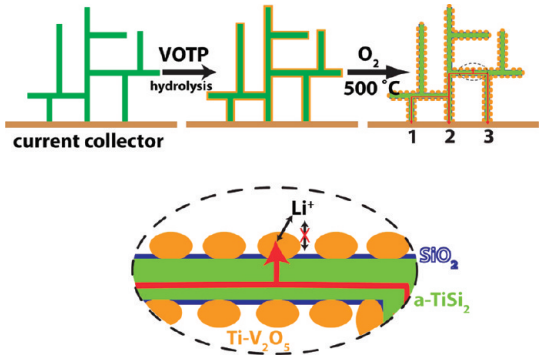

Figure 1. Schematic illustrations of the $TiSi_2/V_2O_5$ heteronanostructure design. The $TiSi_2$ nanonet is directly grown on a current collector; V_2O_5 is deposited onto $TiSi_2$ by a hydrolysis process. Upon annealing at 500 °C in O_2, V_2O_5 nanoparticles form. The interconnectivity of the nanonet provides multiple electron transport pathways to one active site, as indicated by the red arrows that are connected to the current collector at points 1, 2, and 3. The magnified view on the bottom reveals that Li^+ ions specifically react with V_2O_5, whereas electrons primarily travel within $TiSi_2$. The SiO_2 layer produced spontaneously during the annealing step protects $TiSi_2$ from being etched by reactions with Li^+ (see more details in the Supporting Information).

$TiSi_2$ nanonets were synthesized by chemical vapor deposition (CVD) without the involvement of catalysts or growth seeds. The growth was readily carried out on conductive substrates (*e.g.,* Ti foil) that can be used as current collectors, and as such the resulting materials were directly assembled into coin cells for battery characterizations without the need for binders or other additives. The deposition of vanadium precursor, triisopropoxyvandium(V) oxide (VOTP), is a variant of the sol–gel method, which is straightforward to implement.[24] Upon calcination at 500 °C in O_2, discrete nanoparticles (typically 20–30 nm in diameters) formed (Figure 2). They were identified as Ti-doped V_2O_5 (~5% Ti) by elemental analysis (Supporting Information, Figure S1). The Ti came from the $TiSi_2$ nanonets, whose top surface layers were converted to SiO_2 by calcination in the absence of VOTP (Supporting Information, Figures S1 and S6). The SiO_2 coating plays an extremely important role in protecting the conductive framework, as will be discussed later. It is noted that despite the existence of the SiO_2 layer, the electrical resistance between V_2O_5 nanoparticles and $TiSi_2$ core is low, <100 Ω as measured by impedance spectroscopy (Supporting Information, Figure S3). We suggest that SiO_2 only forms on the bare surfaces of $TiSi_2$ but not between V_2O_5 and $TiSi_2$, and as such V_2O_5 particles make direct electrical contact with $TiSi_2$. This hypothesis is supported by high-resolution transmission electron microscopy (HRTEM) as shown in Figure 2c, where no obvious SiO_2 layer exists between the top V_2O_5 particle and $TiSi_2$. That the layer shows up between the bottom right particle and $TiSi_2$ is because the particle mostly resides behind the $TiSi_2$ beam. In other words, it is a viewing angle artifact. This understanding is also manifested in the magnified view of Figure 1 in which we draw V_2O_5 in direct contact with $TiSi_2$. Although the crystalline nanonets were

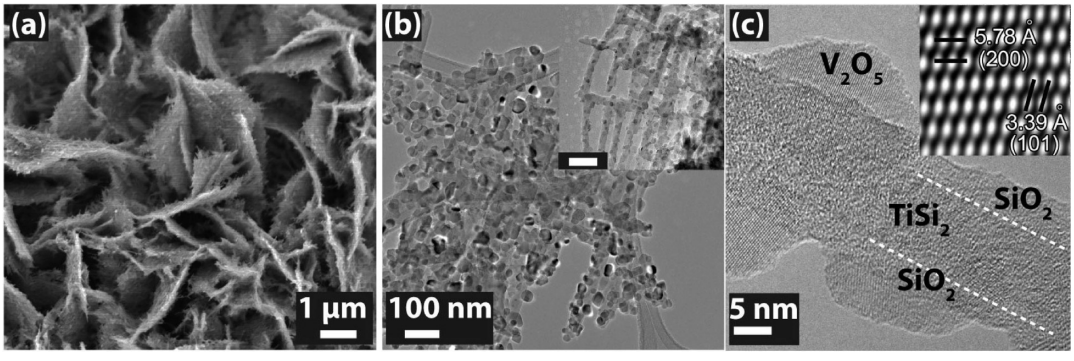

Figure 2. Electron micrographs of $TiSi_2/V_2O_5$ heteronanostructures. (a) Top-view scanning electron micrograph (SEM) of the heteronanostructures showing the high yield of the nanonets, supporting that this approach can produce high content of active materials. (b) Low magnification transmission electron micrograph (TEM) demonstrating the particulate nature of V_2O_5 coating and the interconnectivity of $TiSi_2$ naonets. Because the nanonet morphology is less obvious with regular loading of the V_2O_5 (mainframe), we show the nanostructures at reduced loading of the V_2O_5 in the inset (scale bar: 100 nm; with ~30% less V_2O_5 loading than that in the mainframe). (c) High magnification TEM revealing the details of the heteronanostructure, where an amorphous SiO_2 layer is present (portions of the interface between $TiSi_2$ and SiO_2 highlighted by white dotted lines). The resulting V_2O_5 is highly crystalline (inset). To better study the microstructure of V_2O_5, this HRTEM image was taken on a low-loading $TiSi_2/V_2O_5$ sample, the same as the inset in panel b.

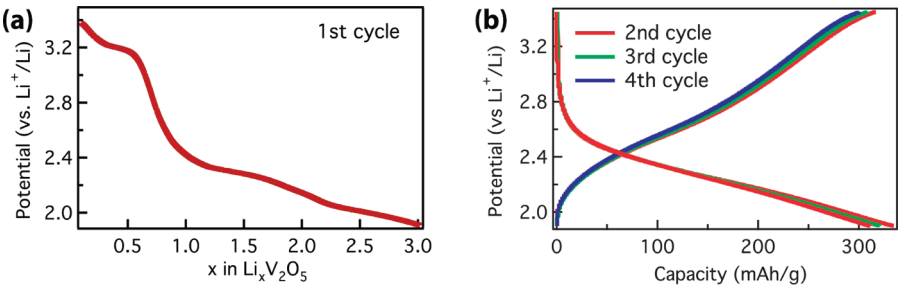

Figure 3. Charge and discharge characteristics of $TiSi_2/V_2O_5$ heteronanostructures. (a) The first cycle of discharge (lithiation) is characteristic of crystalline V_2O_5. Rate of measurement: 60 mA/g. (b) Afterward, V_2O_5 is amorphous, as confirmed by the charge/discharge behaviors. Rate: 540 mA/g.

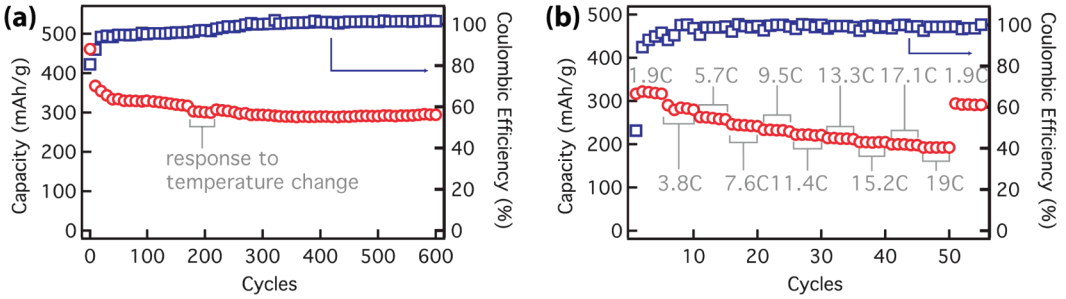

Figure 4. Charge capacity and Coulombic efficiency $TiSi_2/V_2O_5$ heteronanostructures. (a) After the initial decay during the first 40 cycles, the heteronanostructure exhibits remarkable stability for up to 600 cycles, fading only 12% (rate: 300 mA/g). Also worth noting is the reversible decrease of capacity between the 180th and 210th cycles (14 mAh/g, or 4.4%) as a result of controlled temperature change from 30.0 to 28.0 °C (see Supporting Information). For clarity, one data point for every 10 cycles is shown. (b) The rate-dependent specific capacities. 1C: 350 mA/g.

transformed into amorphous during calcination, the nanonet morphology was preserved. More important, the conductivity of amorphous $TiSi_2$ (4×10^3 S/cm)[25] is several orders of magnitude of that of V_2O_5 (*ca.* 10^{-3}–10^{-2} S/cm),[26] thereby enabling a high power rate that has not been measured on V_2O_5 alone. Finally, we note that impedance measurements confirmed the Li^+ diffusion coefficient within the $TiSi_2/V_2O_5$ nanostructures (10^{-13} to 10^{-12} cm^2/s) is similar to that in bulk V_2O_5 (Supporting Information, Figure S4).[27] The thinness of the V_2O_5 coating (typically <30 nm), however, does allow for complete lithiation and/or delithiation of the active material in a short period of time (<90 s), thereby enabling high power rates.

The successful implementation of our approach can produce a cathode material with both high capacity (at 441 mAh/g, V_2O_5 exhibits one of the highest specific capacities as a stable cathode compound) and high power.[28,29] In a typical $TiSi_2/V_2O_5$ nanostructure, the mass of V_2O_5 accounts for *ca.* 80% of the total mass as measured by elemental analysis (Supporting Information), resulting in a theoretical capacity of 350 mAh/g for the overall nanostructure. The first test we conducted was to examine how the $TiSi_2/V_2O_5$ nanostructures behave in a coin cell configuration. At a rate of 60 mA/g (*ca.* 0.2*C*; 1*C* = 350 mA/g), the material exhibited discharge (lithiation; Figure 3a) and charge (delithiation; Supporting Information, Figure S2) behaviors characteristic of that by V_2O_5. The lithiation process took place within the potential window of 3.45 and 1.9 V. The plateau at 3.2 V corresponds to the intercalation of the first Li^+, namely the transformation from the α-($Li_xV_2O_5$, $x < 0.1$) to the ε-($0.35 < x < 0.7$) and then finally the δ-phases ($0.9 < x \leq 1$). Those at 2.3 and 2.0 V correspond to the formation of $Li_2V_2O_5$, and $Li_3V_2O_5$, respectively.[30] The end product of the first lithiation process was ω-$Li_3V_2O_5$, which then underwent reversible lithiation and delithiation as shown in Figure 3b.[31] The result is important because it proves that the addition of $TiSi_2$ does not alter the chemical properties of V_2O_5 to a measurable extent. It is worth noting an initial discharge capacity of 461 mAh/g, higher than the aforementioned limit (350 mAh/g), was measured presumably due to the irreversible processes such as the solid–electrolyte–interface (SEI) layer formation. Consistent with this result was the relatively low Coulombic efficiencies during the initial cycles (81% for the first cycle), which gradually reached a level >99% after 200 cycles. Similar higher than theoretical limit first cycle capacities have been measured on V_2O_5 previously.[28,32] As shown in Figure 3b, the discharge capacity during the second cycle dropped to below 350 mAh/g, indicating the completion of the interfacial processes that resulted in the unusually high initial capacities.

With this understanding established, we next sought to observe how the nanostructures behave upon prolonged charge/discharge. For this test, we set the

rate at *ca*. 0.9*C* (300 mA/g, Figure 4a). After the initial decrease during the first 40 cycles from 461 mAh/g (first cycle only) to 334 mAh/g, the capacity remained stable during the remainder of the test for up to 600 cycles, fading only 12%. It corresponds to an average capacity decrease of 0.023% per cycle, a remarkable value considering that the test was carried out at a reasonably fast rate. The $TiSi_2/V_2O_5$ nanostructures were also examined at different charge/discharge rates, and the results were plotted in Figure 4b. At 19*C* (6650 mA/g), the measured capacity of 192 mAh/g corresponds to a discharge power rate of 14.5 kW/kg (see Supporting Information for details of the calculation), one of the highest measured on V_2O_5-based cathode materials. Equally important to potential practical applications, greater than 93% of the initial capacity was recovered when the cell was measured at 1.9*C* again after the varying-rates measurements.

The high capacity at high charge/discharge rates inspired us to examine the stability of $TiSi_2/V_2O_5$ nanostructures after extended charge/discharge cycles at relatively fast rates. Figure 5 shows the remarkable stability of $TiSi_2/V_2O_5$ at a rate of 25*C*, where a specific capacity of 168 mAh/g was measured. We note although cathode materials exhibiting higher power rates[3,4,33] *or* higher capacities[34] have been separately reported, one that shows combined high power *and*

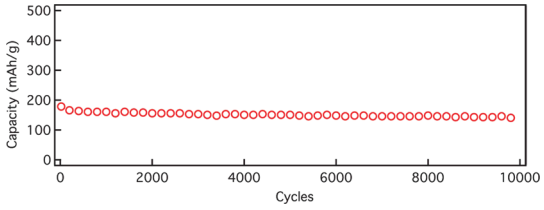

Figure 5. At the rate of 25*C*, an initial specific capacity of 168 mAh/g is measured; this value is 132 mAh/g after 9800 cycles of repeated charge/discharge, corresponding to a capacity retention of 78.7%. For clarity, one data point for every 200 cycles is shown here. Coulombic efficiency is maintained at >99% during the test (not shown for clarity reasons).

high capacity as our $TiSi_2/V_2O_5$ nanostructures do is absent in the literature except for devices made of thin films.[35,36] The $TiSi_2/V_2O_5$ nanostructures reported here are fundamentally different from thin films in the loading densities of active materials. Because the overall dimensions of the $TiSi_2$ nanonets are in the micrometer range, and the nanonets naturally grow into packed structures, the density of activity materials can be comparable to other powder-based technologies. For all measurements conducted in this report, the packing density of $TiSi_2$ nanonets was not optimized. Yet we already achieved an areal density of up to 2 mg/cm^2. It is highly conceivable that we should be able to improve it further through growth optimizations. As such our result represents a major advancement in the field of lithium ion research.

To understand what enables the high performance, we characterized the nanostructures by TEM after 1500 cycles of repeated charge/discharge and found the overall nanonet configuration remained except that the crystalline V_2O_5 nanoparticles turned amorphous due to the initial lithiation process (Figure 6c). We suggest the Ti-doping within V_2O_5 plays a positive role in stabilizing the active material upon lithiation and delithiation because the cycling stability as shown in Figure 5 has not been previously reported on V_2O_5 without doping, to the best of our knowledge. This hypothesis is in line with existing literature that the addition of Ti improves the cycling stability of V_2O_5 system. However, a detailed mechanism by which the effect functions remains a topic of debates.[37−39] For instance, Davies *et al*. argue that the improvement is due to the preferential reduction of Ti^{4+} to Ti^{3+} at low potential, which prevents the reorganization of the structure,[38] whereas Surca *et al*. propose that the V/Ti-oxide system forms a solid solution with V−O−Ti groups in an amorphous state.[39] The solid-solution model may be more suitable to explain the observed stability in our system because the TEM studies did reveal that the V_2O_5 coating was amorphous after lithation/delithation. Clearly more research is needed

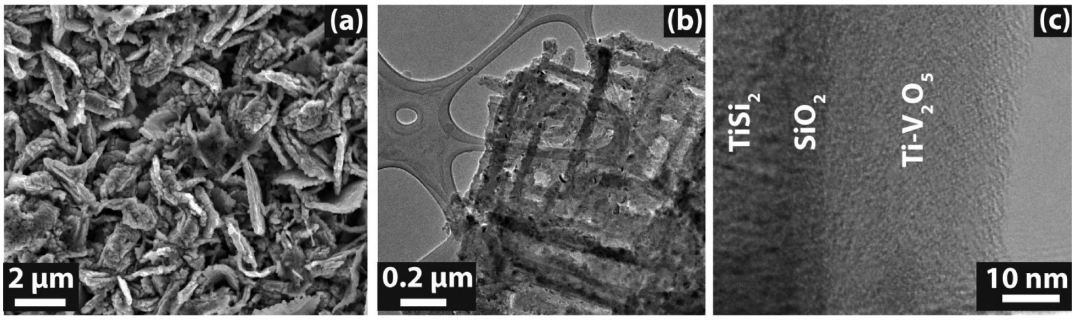

Figure 6. $TiSi_2/V_2O_5$ heteronanostructures after 1500 cycles of repeated charge/discharge. (a) An SEM image showing the overall morphology of the electrode material remains unchanged after the prolonged test. (b) A low magnification TEM image revealing the interconnectivity of the $TiSi_2$ nanonet is maintained, proving that the nanonet is preserved during the charge/discharge process. The particulate nature of V_2O_5 as shown in Figure 2 is no longer obvious as the repeated lithiation/delithiation processes have turned V_2O_5 amorphous. (c) A high magnification TEM image further confirming the $TiSi_2$ core is protected. The V_2O_5 nanoparticles, now amorphous and in a form of continuous films, remain connected to the nanonets.

to fully understand how Ti is distributed in the V_2O_5/$TiSi_2$ system and how it affords the excellent stability. It is noted that TiO_2 does not participate in the reactions within the voltage range of 3.45 to 2 V, ruling out potential contributions from oxides other than V_2O_5 in the system. Significantly, the $TiSi_2$ core and SiO_2 protection coating were intact after the extended test. Control experiments revealed that the SiO_2 was critical to the measured stability, without which the $TiSi_2$ nanonet morphology was nearly indistinguishable after 175 cycles (Supporting Information). That morphological degradation was accompanied by capacity decrease, further confirming that maintaining a highly conductive core in its intact form is the key to the high stability as reported here.

CONCLUSIONS

A novel $TiSi_2/V_2O_5$ heteronanostructure based on the unique nanonet platform was achieved. It showed excellent performance as lithium ion battery cathode, where the active material was Ti-doped V_2O_5, and $TiSi_2$ nanonets act as structural support and charge transporter. Ti-doping stabilizes V_2O_5, and a thermal annealing induced SiO_2 layer shields $TiSi_2$ from the electrolyte. More critically, the unique two-dimensional nanonet platform bridges different length scales from the nanoscale to the micro/macro scale. By introducing a dedicated charge transporter, we were able to separate charge and ionic behaviors and thereby obtain unprecedented high power *and* high capacity on a cathode material that can be cycled extensively. We emphasize our strategy is highly modular, and other high performance cathode compounds (such as $LiFePO_4$) should be readily integrated into the nanonet-based design. Our results demonstrated that advanced functional materials can be obtained by simple chemical synthesis. This approach should be highly complementary to existing efforts of finding highly performing compounds as battery electrode materials.

EXPERIMENTAL SECTION

$TiSi_2$ Synthesis. $TiSi_2$ nanonets were synthesized by chemical vapor deposition (CVD) following previously published procedures.[7] Briefly, 50 sccm (standard cubic centimeter per minute) SiH_4 (10% in He; Airgas), and 2 sccm $TiCl_4$ (Sigma-Aldrich, 98%) carried by 100 sccm H_2 (Airgas) were delivered into the growth chamber, which was heated to 675 °C and kept at 5 Torr during the growth. A Ti foil (Sigma-Aldrich; 0.127 mm) was used as the receiving substrate and subsequently as the current collector for coin cell fabrications. After 12 min of reactions, the supply of SiH_4 was cut off while $TiCl_4$ and H_2 flow was maintained for 3 min. The sample was then transferred into an Ar-filled glovebox (Vacuum Atmosphere Co.) for V_2O_5 deposition.

V_2O_5 Deposition. V_2O_5 deposition was carried out in a glovebox, where a drop (3 μL) of isopropoxyvanadium(V) oxide (VOTP; Strem Chemical, > 98%) was applied on the surface of $TiSi_2$ nanonets (1 × 1 cm^2) by a syringe. Afterward, the sample was allowed to age within the glovebox for 12 h, during which time VOTP reacted with the trace amount of moisture (<5 ppm) within the glovebox to undergo hydrolysis. This slow reaction step was found critical because it led to the formation of a uniform coating of V_2O_5 on $TiSi_2$. Hydrolysis in ambient air produced porous V_2O_5 that behaved poorly in battery characterizations. Once the coating was formed, the sample was brought into ambient air and was heated at 80 °C for 2 h to allow for more complete hydrolysis. This process was repeated for more loading of V_2O_5. It was discovered that two such cycles produced $TiSi_2$ nanostructures with *ca.* 80% (wt%) of V_2O_5. When desired V_2O_5 deposition was achieved, the sample was calcined in dry O_2 at 500 °C for 2 h to conclude the preparation procedure.

Coin Cell Fabrication. CR2032-type coin cells were assembled in the glovebox (O_2 < 2 ppm) using an MTI hydraulic crimping machine (model no. EQ-MSK-110) with a lithium foil as the anode (Sigma; 0.38 mm thick). The electrolyte was $LiPF_6$ (1.0 M) dissolved in ethylene carbonate and diethyl carbonate (1:1 wt/wt; Novolyte Technologies). A polypropylene membrane (25 μm in thickness, Celgard 2500) was used as a separator between the two electrodes.

Battery Characterizations. After assembly, the coin cells were placed in a home-built environmental box with a temperature variation less than ±0.2 °C and measured by a 16-channel battery analyzer station (Neware, China; current range: 1 μA to 1 mA). Data were collected and analyzed using the accompanying software. For all data except those noted, the measurements were conducted at 30 °C. The cyclic voltammetry measurements were performed in a three-electrode configuration with lithium ribbons (Sigma; 1 mm thick) as the counter and reference electrodes, respectively. The working and counter electrodes were rolled together by the separator. All three electrodes were dipped in an electrolyte of the same composition as noted above. The entire setup was kept in a plastic box placed in the glovebox to minimize environmental influences. A CHI 600C potentiostat/galvanostat was used for the measurement (see Supporting Information).

Structural Characterizations. Structural characterizations were performed on a scanning electron microscope (SEM, JEOL 6340F) and a transmission electron microscope (TEM, JEOL 2010F). Elemental analysis was carried out using the energy dispersion spectrometer attached to the TEM.

Acknowledgment. This work was supported by Boston College, and in part by NSF (DMR-1055762). We are grateful to C. H. Kuo's help with Figure 6. We are also grateful for insightful discussions with C. K. Tsung and technical support from Mr. S. Shepard and G. Yuan. The anonymous reviewers of this article also helped us tremendously in improving this work.

Supporting Information Available: Energy dispersive spectrum (EDS) of $TiSi_2/V_2O_5$ heterostructures; delithiation characteristics during the first cycle; electrochemical impedance spectroscopy (EIS) measurement; influence of temperature on capacity; details about power density calculations; TEM data of $TiSi_2$ with and without SiO_2 coating after cycling tests and current−voltage (CV) measurements. This material is available free of charge *via* the Internet at http://pubs.acs.org.

REFERENCES AND NOTES

1. Bruce, P. G.; Scrosati, B.; Tarascon, J.-M. Nanomaterials for Rechargeable Lithium Batteries. *Angew. Chem., Int. Ed.* **2008**, *47*, 2930–2946.
2. Chan, C. K.; Peng, H.; Liu, G.; McIlwrath, K.; Zhang, X. F.; Huggins, R. A.; Cui, Y. High-Performance Lithium Battery Anodes Using Silicon Nanowires. *Nat. Nanotechnol.* **2008**, *3*, 31–35.
3. Kang, B.; Ceder, G. Battery Materials for Ultrafast Charging and Discharging. *Nature* **2009**, *458*, 190–193.

4. Zhang, H.; Yu, X.; Braun, P. V. Three-Dimensional Bicontinuous Ultrafast Charge and Discharge Bulk Battery Electrodes. *Nat. Nanotechnol.* **2011**, *6*, 277–281.
5. Magasinski, A.; Dixon, P.; Hertzberg, B.; Kvit, A.; Ayala, J.; Yushin, G. High-Performance Lithium-Ion Anodes Using a Hierarchical Bottom-up Approach. *Nat. Mater.* **2010**, *9*, 353–358.
6. Ji, X.; Lee, K. T.; Nazar, L. F. A Highly Ordered Nanostructured Carbon-Sulphur Cathode for Lithium-Sulphur Batteries. *Nat. Mater.* **2009**, *8*, 500–506.
7. Cao, A.-M.; Hu, J.-S.; Liang, H.-P.; Wan, L.-J. Self-Assembled Vanadium Pentoxide (V_2O_5) Hollow Microspheres from Nanorods and Their Application in Lithium-Ion Batteries. *Angew. Chem., Int. Ed.* **2005**, *44*, 4391–4395.
8. Zhou, S.; Liu, X. H.; Lin, Y. J.; Wang, D. W. Spontaneous Growth of Highly Conductive Two-Dimensional Single-Crystalline $TiSi_2$ Nanonets. *Angew. Chem., Int. Ed.* **2008**, *47*, 7681–7684.
9. Lee, K.; Cao, G. Enhancement of Intercalation Properties of V_2O_5 Film by TiO_2 Addition. *J. Phys. Chem. B* **2005**, *109*, 11880–11885.
10. Sahana, M. B.; Sudakar, C.; Thapa, C.; Naik, V. M.; Auner, G. W.; Naik, R.; Padmanabhan, K. R. The Effect of Titanium on the Lithium Intercalation Capacity of V_2O_5 Thin Films. *Thin Solid Films* **2009**, *517*, 6642–6651.
11. Zhou, S.; Liu, X.; Wang, D. Si/$TiSi_2$ Heteronanostructures as High-Capacity Anode Material for Li Ion Batteries. *Nano Lett.* **2010**, *10*, 860–863.
12. Winter, M.; Besenhard, J. O. Electrochemical Lithiation of Tin and Tin-Based Intermetallics and Composites. *Electrochim. Acta* **1999**, *45*, 31–50.
13. Yan, J.; Sumboja, A.; Khoo, E.; Lee, P. S. V_2O_5 Loaded on SnO_2 Nanowires for High-Rate Li Ion Batteries. *Adv. Mater.* **2011**, *23*, 746–750.
14. Takahashi, K.; Wang, Y.; Cao, G. Ni-$V_2O_5 \cdot nH_2O$ Core−Shell Nanocable Arrays for Enhanced Electrochemical Intercalation. *J. Phys. Chem. B* **2004**, *109*, 48–51.
15. Rolison, D. R.; Long, J. W.; Lytle, J. C.; Fischer, A. E.; Rhodes, C. P.; McEvoy, T. M.; Bourg, M. E.; Lubers, A. M. Multifunctional 3D Nanoarchitectures for Energy Storage and Conversion. *Chem. Soc. Rev.* **2009**, *38*, 226–252.
16. Lee, S. W.; Kim, J.; Chen, S.; Hammond, P. T.; Shao-Horn, Y. Carbon Nanotube/Manganese Oxide Ultrathin Film Electrodes for Electrochemical Capacitors. *ACS Nano* **2010**, *4*, 3889–3896.
17. Chen, Z.; Augustyn, V.; Wen, J.; Zhang, Y.; Shen, M.; Dunn, B.; Lu, Y. High-Performance Supercapacitors Based on Intertwined CNT/V_2O_5 Nanowire Nanocomposites. *Adv. Mater.* **2011**, *23*, 791–795.
18. Wang, H.; Yang, Y.; Liang, Y.; Cui, L.-F.; Sanchez Casalongue, H.; Li, Y.; Hong, G.; Cui, Y.; Dai, H. $LiMn_{1-x}Fe_xPO_4$ Nanorods Grown on Graphene Sheets for Ultrahigh-Rate-Performance Lithium Ion Batteries. *Angew. Chem., Int. Ed.* **2011**, *50*, 7364–7368.
19. Liu, H.; Yang, W. Ultralong Single Crystalline V_2O_5 Nanowire/Graphene Composite Fabricated by a Facile Green Approach and Its Lithium Storage Behavior. *Energy Environ. Sci.* **2011**, *4*, 4000–4008.
20. Leroux, F.; Koene, B. E.; Nazar, L. F. Electrochemical Lithium Intercalation into a Polyaniline/V_2O_5 Nanocomposite. *J. Electrochem. Soc.* **1996**, *143*, L181–L183.
21. Zhou, S.; Liu, X.; Lin, Y.; Wang, D. Rational Synthesis and Structural Characterizations of Complex $TiSi_2$ Nanostructures. *Chem. Mater.* **2009**, *21*, 1023–1027.
22. Zhou, S.; Wang, D. Unique Lithiation and Delithiation Processes of Nanostructured Metal Silicides. *ACS Nano* **2010**, *4*, 7014–7020.
23. Whittingham, M. S.; Song, Y. N.; Lutta, S.; Zavalij, P. Y.; Chernova, N. A. Some Transition Metal (Oxy)Phosphates and Vanadium Oxides for Lithium Batteries. *J. Mater. Chem.* **2005**, *15*, 3362–3379.
24. Patrissi, C. J.; Martin, C. R. Sol-Gel-Based Template Synthesis and Li-Insertion Rate Performance of Nanostructured Vanadium Pentoxide. *J. Electrochem. Soc.* **1999**, *146*, 3176–3180.
25. Park, D.-G.; Suh, Y.-S.; Lee, S.-H.; Kim, S.-D.; Kim, C.-T. Thermal Stability of Sputter-Deposited $TiSi_2$ Films with Crystal Orientation. *Electrochem. Solid-State Lett.* **1999**, *2*, 642–644.
26. Muster, J.; Kim, G. T.; Krstić, V.; Park, J. G.; Park, Y. W.; Roth, S.; Burghard, M. Electrical Transport through Individual Vanadium Pentoxide Nanowires. *Adv. Mater.* **2000**, *12*, 420–424.
27. McGraw, J. M.; Bahn, C. S.; Parilla, P. A.; Perkins, J. D.; Readey, D. W.; Ginley, D. S. Li Ion Diffusion Measurements in V_2O_5 and $Li(Co_{1-x}Al_x)O_2$ Thin-Film Battery Cathodes. *Electrochim. Acta* **1999**, *45*, 187–196.
28. Dong, W.; Rolison, D. R.; Dunna, B. Electrochemical Properties of High Surface Area Vanadium Oxide Aerogels. *Electrochem. Solid-State Lett.* **2000**, *3*, 457–459.
29. Lee, K. T.; Nazar, L. F. Positive Electrode Materials for Li-Ion and Li-Batteries. *Chem. Mater.* **2010**, *22*, 691–714.
30. Delmas, C.; Cognacauradou, H.; Cocciantelli, J. M.; Menetrier, M.; Doumerc, J. P. The $Li_xV_2O_5$ System—An Overview of the Structure Modifications Induced by the Lithium Intercalation. *Solid State Ionics* **1994**, *69*, 257–264.
31. We note that one practical challenge of using V_2O_5 as cathode is that $Li_xV_2O_5$ is not directly synthesized. However, this challenge may be circumvented by this transformation process, which produces ω-$Li_3V_2O_5$.
32. Wang, Y.; Takahashi, K.; Lee, K.; Cao, G. Z. Nanostructured Vanadium Oxide Electrodes for Enhanced Lithium-Ion Intercalation. *Adv. Funct. Mater.* **2006**, *16*, 1133–1144.
33. Kang, K.; Meng, Y. S.; Breger, J.; Grey, C. P.; Ceder, G. Electrodes with High Power and High Capacity for Rechargeable Lithium Batteries. *Science* **2006**, *311*, 977–980.
34. Ammundsen, B.; Paulsen, J. Novel Lithium-Ion Cathode Materials Based on Layered Manganese Oxides. *Adv. Mater.* **2001**, *13*, 943–956.
35. Lee, S. W.; Gallant, B. M.; Byon, H. R.; Hammond, P. T.; Shao-Horn, Y. Nanostructured Carbon-Based Electrodes: Bridging the Gap between Thin-Film Lithium-Ion Batteries and Electrochemical Capacitors. *Energy Environ. Sci.* **2011**, *4*, 1972–1985.
36. Liu, Y.; Clark, M.; Zhang, Q.; Yu, D.; Liu, D.; Liu, J.; Cao, G. V_2O_5 Nano-Electrodes with High Power and Energy Densities for Thin Film Li-Ion Batteries. *Adv. Energy Mater.* **2011**, *1*, 194–202.
37. Minett, M. G.; Owen, J. R. Vanadium and Titanium Oxides Prepared by Hydrolysis of Alkoxides as Insertion Electrodes in Lithium Cells with Polymeric Electrolytes. *J. Power Sources* **1990**, *32*, 81–97.
38. Davies, A.; Hobson, R. J.; Hudson, M. J.; Macklin, W. J.; Neat, R. J. Sol-Gel-Derived Vanadium and Titanium Oxides as Cathode Materials in High-Temperature Lithium Polymer-Electrolyte Cells. *J. Mater. Chem.* **1996**, *6*, 49–56.
39. Šurca, A.; Benčič, S.; Orel, B.; Pihlar, B. Spectroelectrochemical Studies of V/Ti−, V/Ti/Zr−, and V/Ti/Ce−Oxide Counter-Electrode Films. *Electrochim. Acta* **1999**, *44*, 3075–3084.